J|A|C|S
ARTICLES
Published on Web 03/10/2006

Mechanism of $Pd(OAc)_2$/DMSO-Catalyzed Aerobic Alcohol Oxidation: Mass-Transfer-Limitation Effects and Catalyst Decomposition Pathways

Bradley A. Steinhoff and Shannon S. Stahl*

Contribution from the Department of Chemistry, University of Wisconsin—Madison, 1101 University Avenue, Madison, Wisconsin 53706

Received November 22, 2005; E-mail: stahl@chem.wisc.edu

Abstract: $Pd(OAc)_2$ in DMSO is an effective catalyst for the aerobic oxidation of alcohols and numerous other organic substrates. Kinetic studies of the catalytic oxidation of primary and secondary benzylic alcohol substrates provide fundamental insights into the catalytic mechanism. In contrast to the conclusion reached in our earlier study (*J. Am. Chem. Soc.* **2002**, *124*, 766−767), we find that Pd(II)-mediated alcohol oxidation is the turnover-limiting step of the catalytic reaction. At elevated catalyst loading, however, the rate of catalytic turnover is limited by the dissolution of oxygen gas into solution. This mass-transfer rate is measured directly by using gas-uptake methods, and it correlates with the maximum rate observed during catalysis. Initial-rate studies were complemented by kinetic analysis of the full-reaction timecourses at different catalyst concentrations. Kinetic fits of these traces reveal the presence of unimolecular and bimolecular catalyst decomposition pathways that compete with productive catalytic turnover.

Introduction

Palladium-catalyzed oxidation reactions rank among the most versatile strategies for the selective oxidation of organic molecules with molecular oxygen. Effective transformations range from alcohol oxidation and oxidative carbonylation reactions to oxidative C−C, C−O, and C−N coupling reactions with alkenes.[1] The Wacker process (eq 1), discovered in the late 1950s,[2] represents the most prominent example of this reaction class; however, substantial advances have occurred over the past decade. The recent developments can be linked to the discovery that coordinating solvents and oxidatively stable ligands enable dioxygen-coupled catalytic turnover to be achieved in the absence of cocatalytic and/or stoichiometric oxidants such as benzoquinone and copper(II) chloride. The Pd-$(OAc)_2$/DMSO catalyst system, discovered independently by the groups of Larock and Hiemstra in the mid-1990s, was among the first breakthroughs in this area.[3,4] Although earlier examples of cocatalyst-free aerobic oxidation reactions were known,[5] this catalyst system was the first to find broad applicability to a wide range of organic oxidation reactions (e.g., eqs 2−5).

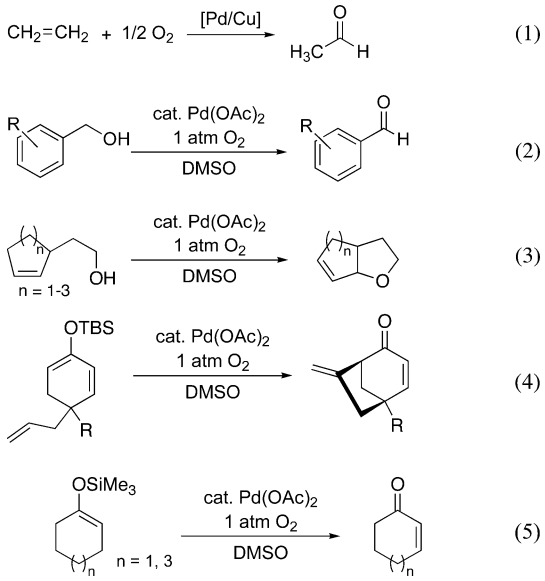

Numerous additional catalyst systems have been reported subsequently (Chart 1), particularly for application to aerobic alcohol oxidation.[6] The catalytic mechanism of these reactions features an oxidase-style sequence consisting of two half reactions: substrate oxidation by palladium(II) followed by aerobic oxidation of the reduced catalyst (steps *i* and *ii*, Scheme 1).[1a] Mechanistic studies have illuminated important fundamental steps associated with these half reactions,[7] and it is evident

(1) For recent review articles and accounts, see the following: (a) Stahl, S. S. *Science* **2005**, *309*, 1824−1826. (b) Stahl, S. S. *Angew. Chem., Int. Ed.* **2004**, *43*, 3400−3420. (c) Sheldon, R. A.; Arends, I. W. C. E.; ten Brink, G.-J.; Dijksman, A. *Acc. Chem. Res.* **2002**, *35*, 774−781. (d) Stoltz, B. M. *Chem. Lett.* **2004**, *33*, 362−367. (e) Sigman, M. S.; Schultz, M. J. *Org. Biomol. Chem.* **2004**, *2*, 2551−2554. (f) Toyota, M.; Ihara, M. *Synlett* **2002**, 1211−1222. (g) Nishimura, T.; Uemura, S. *Synlett* **2004**, 201−216.

(2) Smidt, J.; Hafner, W.; Jira, R.; Sedlmeier, J.; Sieber, R.; Rüttinger, R.; Kojer, H. *Angew. Chem.* **1959**, *71*, 176−182.

(3) For leading references, see: (a) Larock, R. C.; Hightower, T. R. *J. Org. Chem.* **1993**, *58*, 5298−5300. (b) van Benthem, R. A. T. M.; Hiemstra, H.; Michels, J. J.; Speckamp, W. N. *J. Chem. Soc., Chem. Commun.* **1994**, 357−359. (c) van Benthem, R. A. T. M.; Hiemstra, H.; Longarela, G. R.; Speckamp, W. N. *Tetrahedron Lett.* **1994**, *35*, 9281−9284. (d) Larock, R. C.; Hightower, T. R.; Kraus, G. A.; Hahn, P.; Zheng, D. *Tetrahedron Lett.* **1995**, *36*, 2423−2426. (e) van Benthem, R. A. T. M.; Hiemstra, H.; van Leeuwen, P. W. N. M.; Geus, J. W.; Speckamp, W. N. *Angew. Chem., Int. Ed. Engl.* **1995**, *34*, 457−460. (f) Larock, R. C.; Hightower, T. R.; Hasvold, L. A.; Peterson, K. P. *J. Org. Chem.* **1996**, *61*, 3584−3585. (g) Peterson, K. P.; Larock, R. C. *J. Org. Chem.* **1998**, *63*, 3185−3189.

10.1021/ja057914b CCC: $33.50

Chart 1. Catalyst Systems that Promote Direct Dioxygen-Coupled Oxidation of Organic Substrates

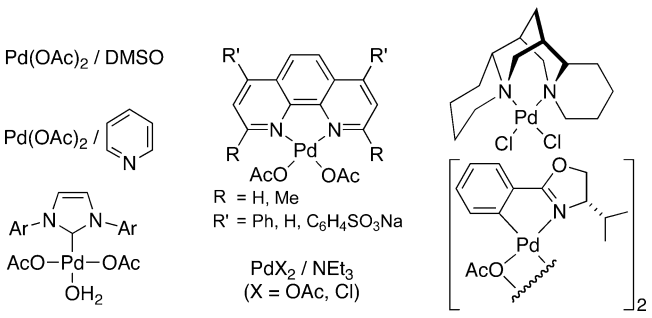

from these studies that the ligands coordinated to palladium exert a significant influence on the reaction, including the rate (turnover frequency), the nature of the catalyst resting state, and the identity of the turnover-limiting step. Ligands also influence the catalyst stability by affecting the rate of catalyst reoxidation relative to decomposition (steps *ii* and *iii*, Scheme 1).

$Pd(OAc)_2$/DMSO is the only catalyst system for which aerobic oxidation of the catalyst (step *ii*, Scheme 1) has been reported to be the turnover-limiting step.[7a,8] In all other systems, steps associated with palladium(II)-mediated oxidation of the alcohol are turnover limiting (step *i*, Scheme 1).[7] In the current study, we present a more thorough kinetic analysis of $Pd(OAc)_2$/DMSO-catalyzed aerobic alcohol oxidation that reveals this catalyst system is susceptible to mass-transfer-limited rates under conditions commonly employed for synthetic reactions. Namely, the catalytic rate can be controlled by the rate of oxygen gas dissolution into DMSO. If an adequate supply of dioxygen is available in solution, the $Pd(OAc)_2$/DMSO system also exhibits turnover-limiting alcohol oxidation by palladium(II). Because palladium(0) is an intrinsically unstable form of the catalyst (cf. Scheme 1), slow dissolution of oxygen into the reaction mixture not only limits the reaction rate but also leads to enhanced catalyst decomposition. Mechanistic insights into catalyst decomposition pathways are obtained from analysis of the full kinetic timecourses of catalytic reactions. The results of this study and the methods described herein are applicable to the entire scope of palladium-catalyzed aerobic oxidation reactions.

Scheme 1. General Mechanism of Palladium-Catalyzed Aerobic Alcohol Oxidation

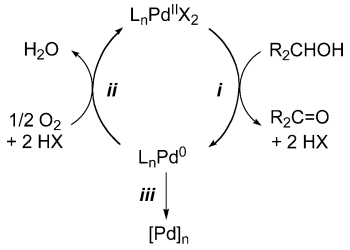

Results and Discussion

Kinetic Studies of Alcohol Oxidation. Our initial mechanistic studies of the $Pd(OAc)_2$/DMSO system focused on the oxidation of 2,5-dimethoxybenzyl alcohol, **1**.[7a] This reaction, originally reported by Peterson and Larock,[3g] proceeds to nearly complete conversion within 12 h at 80 °C (eq 6). In our earlier

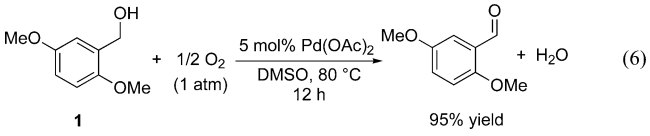

(6)

study, we demonstrated that the reaction stoichiometry corresponds to an O_2/substrate ratio of 0.50(3). Control experiments reveal that hydrogen peroxide, if it forms in the reaction, is not competent to serve as an oxidant because it undergoes rapid disproportionation in the presence of the palladium catalyst.[9]

Kinetic studies of the catalytic reaction were performed by using a computer-interfaced gas-uptake apparatus to monitor the change in oxygen pressure within in a sealed, temperature-controlled reaction vessel. The lack of an induction period enabled us to obtain much of our kinetics data via initial-rate methods. Analysis of the full-reaction timecourse provides additional insights into the catalytic mechanism (see below).

The dependence of the rate on $[Pd(OAc)_2]$ displays a nonlinear correlation that fits well to a hyperbolic function (saturation-like kinetics). The curve-fit asymptotically approaches a maximum rate of 126 μmol/min (Figure 1A). The

(4) Other groups have also employed the $Pd(OAc)_2$/DMSO catalyst system in aerobic oxidation reactions. See, for example: (a) Ref 1f. (b) Rönn, M.; Bäckvall, J.-E.; Andersson, P. G. *Tetrahedron Lett.* **1995**, *36*, 7749−7752. (c) Rönn, M.; Andersson, P. G.; Bäckvall, J.-E. *Acta Chem. Scand.* **1997**, *51*, 773−777. (d) Bee, C.; Leclerc, E.; Tius, M. A. *Org. Lett.* **2003**, *5*, 4927−4930.

(5) See, for example: (a) Davidson, J. M.; Triggs, C. *Chem. Ind.* **1967**, 1361. (b) Itatani, H.; Yoshimoto, H. *Chem. Ind.* **1971**, 674−675. (c) Blackburn, T. F.; Schwartz, J. *J. Chem. Soc., Chem. Commun.* **1977**, 157−158. (d) Hosokawa, T.; Miyagi, S.; Murahashi, S.; Sonoda, A. *J. Org. Chem.* **1978**, *43*, 2752−2757.

(6) See review articles in ref 1 and the following leading references: $Pd(OAc)_2$/pyridine: (a) Nishimura, T.; Onoue, T.; Ohe, K.; Uemura, S. *J. Org. Chem.* **1999**, *64*, 6750−6755. (b) Iwasawa, T.; Tokunaga, M.; Obora, Y.; Tsuji, Y. *J. Am. Chem. Soc.* **2004**, *126*, 6554−6555. $Pd(OAc)_2$/phenanthroline derivatives: (c) ten Brink, G.-J.; Arends, I. W. C. E.; Sheldon, R. A. *Science* **2000**, *287*, 1636−1639. (d) Bianchi, D.; Bortolo, R.; D'Aloisio, R.; Ricci, M. *Angew. Chem., Int. Ed.* **1999**, *38*, 706−708. $PdCl_2$/(−)-sparteine: (e) Ferreira, E. M.; Stoltz, B. M. *J. Am. Chem. Soc.* **2001**, *123*, 7725−7726. (f) Jensen, D. R.; Pugsley, J. S.; Sigman, M. S. *J. Am. Chem. Soc.* **2001**, *123*, 7475−7476. PdX_2/NEt_3: (g) Schultz, M. J.; Park, C. C.; Sigman, M. S. *Chem. Commun.* **2002**, 3034−3035. (h) Timokhin, V. I.; Anastasi, N. R.; Stahl, S. S. *J. Am. Chem. Soc.* **2003**, *125*, 12996−12997. (NHC)Pd-$(OAc)_2(OH_2)$: (i) Jensen, D. R.; Schultz, M. J.; Mueller, J. A.; Sigman, M. S. *Angew. Chem., Int. Ed.* **2003**, *42*, 3810−3813. Palladacycles: (j) Hallman, K.; Moberg, C. *Adv. Synth. Catal.* **2001**, *343*, 260−263.

(7) For mechanistic studies of catalytic aerobic alcohol oxidation with different catalyst systems, see the following. $Pd(OAc)_2$/DMSO: (a) Steinhoff, B. A.; Fix, S. R.; Stahl, S. S. *J. Am. Chem. Soc.* **2002**, *124*, 766−767. Pd-$(OAc)_2$/pyridine: (b) Steinhoff, B. A.; Stahl, S. S. *Org. Lett.* **2002**, *4*, 4179−4181. (c) Steinhoff, B. A.; Guzei, I. A.; Stahl, S. S. *J. Am. Chem. Soc.* **2004**, *126*, 11268−11278. $Pd(OAc)_2$/phenanthroline derivatives: (d) ten Brink, G.-J.; Arends, I. W. C. E.; Sheldon, R. A. *Adv. Synth. Catal.* **2002**, *344*, 355−369. (e) ten Brink, G.-J.; Arends, I. W. C. E.; Hoogenraad, M.; Verspui, G.; Sheldon, R. A. *Adv. Synth. Catal.* **2003**, *345*, 497−505. (f) ten Brink, G.-J.; Arends, I. W. C. E.; Hoogenraad, M.; Verspui, G.; Sheldon, R. A. *Adv. Synth. Catal.* **2003**, *345*, 1341−1352. (g) Bortolo, R.; Bianchi, D.; D'Aloisio, R.; Querci, C.; Ricci, M. *J. Mol. Catal. A* **2000**, *153*, 25−29. $PdCl_2$/(−)-sparteine: (h) Mueller, J. A.; Jensen, D. R.; Sigman, M. S. *J. Am. Chem. Soc.* **2002**, *124*, 8202−8203. (i) Mueller, J. A.; Sigman, M. S. *J. Am. Chem. Soc.* **2003**, *125*, 7005−7013. (j) Trend, R. M.; Stoltz, B. M. *J. Am. Chem. Soc.* **2004**, *126*, 4482−4483. $Pd(OAc)_2$/NEt_3: (k) Schultz, M. J.; Adler, R. S.; Zierkiewicz, W.; Privalov, T.; Sigman, M. S. *J. Am. Chem. Soc.* **2005**, *127*, 8499−8507. (NHC)$Pd(OAc)_2(OH_2)$: (l) Mueller, J. A.; Goller, C. P.; Sigman, M. S. *J. Am. Chem. Soc.* **2004**, *126*, 9724−9734. Palladacycles: (m) Paavola, S.; Zetterberg, K.; Privalov, T.; Csöregh, I.; Moberg, C. *Adv. Synth. Catal.* **2004**, *346*, 237−244.

(8) For a recent computational study of the $Pd(OAc)_2$/DMSO system, see: Zierkiewicz, W.; Privalov, T. *Organometallics* **2005**, *24*, 6019−6028.

(9) For a detailed description of the control experiments used to establish this fact, see the Supporting Information of ref 7a. The precise mechanism of disproportionation is not known; however, we have made the following qualitative observations. Addition of aqueous hydrogen peroxide (30%) to a fresh solution of $Pd(OAc)_2$ (recrystallized from toluene) in DMSO results in rapid disproportionation. In contrast, if hydrogen peroxide is added to a suspension of palladium black obtained from a completed catalytic reaction, disproportionation is slow. These observations suggest that the Pd-catalyzed disproportionation mechanism may proceed via a Pd(II)/Pd(IV) cycle.

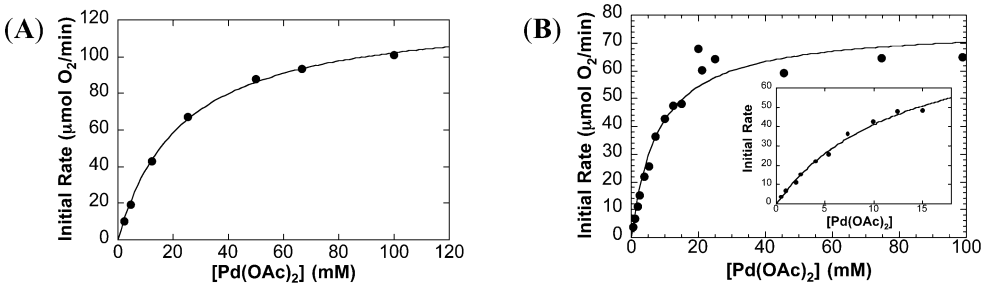

Figure 1. Dependence of the initial rate on $[Pd(OAc)_2]$ for the oxidation of primary alcohol, **1**, in two different reaction vessels: (A) 25 mL round-bottom flask and (B) 25.4 mm OD high-pressure glass reaction tube. Conditions: (A) 2.2−100 mM $Pd(OAc)_2$, 745 Torr O_2, 0.52 M 2,5-dimethoxybenzyl alcohol, 2 mL of DMSO, 80 °C, data fit to a hyperbolic function; (B) 0.48−98.9 mM $Pd(OAc)_2$, 725 Torr O_2, 520 mM 2,5-dimethoxybenzyl alcohol, 2 mL of DMSO, 80 °C, data fit to a hyperbolic function.

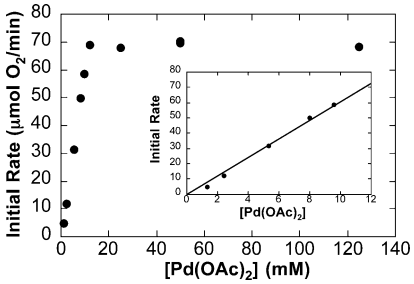

Figure 2. Dependence of the initial rate on $[Pd(OAc)_2]$ for the oxidation of secondary alcohol, **2**. Inset: region in which the rate dependence is first order on [Pd]. Conditions: 1.3−125 mM $Pd(OAc)_2$, 735 Torr O_2, 0.52 M 1-phenylethanol, 2 mL of DMSO, 80 °C, in 25.4 mm OD high-pressure tube.

[Pd(OAc)] dependence differs somewhat if the identical reactions are conducted in a different reaction vessel, namely, a 25.4 mm OD high-pressure glass reaction tube instead of a 25 mL round-bottom flask (Figure 1B). Again, a hyperbolic function fits the data reasonably well; however, some scatter is evident in the data above ~18 mM $Pd(OAc)_2$, and in this case, the fit predicts a maximum rate of only 76 μmol/min.

Subsequent kinetic studies of $Pd(OAc)_2$/DMSO-catalyzed oxidation of 1-phenylethanol, **2** (eq 7), provided valuable additional insights. For this reaction, the $[Pd(OAc)_2]$-dependence

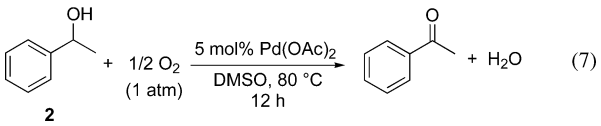

(7)

plot reveals a sharp discontinuity at 12 mM $Pd(OAc)_2$ (Figure 2). Above this concentration, the reaction rate is invariant with respect to $[Pd(OAc)_2]$. The rate plateau observed in these studies (70 μmol/min) is comparable to the maximum rate observed for the oxidation of the primary alcohol **1** in the same reaction vessel (high-pressure reaction tube; Figure 1B). In contrast to the data obtained for the oxidation of **1** (Figure 1), no curvature is evident in the data for the oxidation of **2** at low [Pd] (see inset, Figure 2).

On the basis of these results, we performed additional kinetic studies on the oxidation of **1** and **2** at two different concentrations of $Pd(OAc)_2$. In the oxidation of **1**, reactions conducted at low catalyst loading (0.5 mol %, or 2.5 mM, $Pd(OAc)_2$) reveal that the rate is virtually independent of the oxygen pressure and exhibits a saturation dependence on [alcohol] (Figure 3A,B). Similar measurements were obtained at higher catalyst loading (5 mol %, or 25 mM, $Pd(OAc)_2$), conditions commonly employed for synthetic reactions and in the range of $[Pd(OAc)_2]$ that yields the maximum rate. Under these conditions, the reaction rate exhibits a first-order dependence on the oxygen pressure and is invariant with respect to [alcohol] (Figure 3C,D).

Similar kinetic studies were performed for the oxidation of secondary alcohol **2** at low and high catalyst loading (2.5 and 25 mM, respectively), and identical trends emerged (Supporting Information, Figure S1). At low $[Pd(OAc)_2]$, the reaction rate exhibits an approximately zero-order dependence on the oxygen pressure and a saturation dependence on [alcohol], and at high $[Pd(OAc)_2]$, the rate exhibits a first-order dependence on oxygen pressure and a zero-order dependence on [alcohol].

Characterization of Mass-Transfer-Limited Conditions. The data described above suggest that reactions conducted at high catalyst loading might experience rate-limiting mass-transfer of oxygen gas into solution. Data consistent with mass-transfer-limitation effects include (1) the invariance of the rate on $[Pd(OAc)_2]$ above a threshold concentration, (2) the first-order dependence of the rate on oxygen pressure, and (3) the dependence of the maximum rate on the identity of the reaction vessel under otherwise identical conditions (Figure 1 and Table 1).[10] Additional studies provided further support for this conclusion. At high catalyst loading (25 mM $Pd(OAc)_2$), the initial rate of the catalytic reaction exhibits a linear dependence on the stirring frequency (closed circles, Figure 4). At low catalyst loading (2.5 mM $Pd(OAc)_2$), no stir-rate dependence is observed if stirring is maintained at ≥2000 rpm. Below this value, however, a linear dependence of the rate on stirring frequency is observed. Thus, even at low catalyst concentration, the reaction rate is susceptible to mass-transfer limitations if inadequate agitation is provided.

Under mass-transfer-limiting conditions, the dissolved gas concentration approaches zero because the chemical reaction depletes the gaseous substrate from solution faster than it can be replenished (eq 8).

$$\text{Gas (g)} \underset{-k_L(\text{area})}{\overset{k_L(\text{area})}{\rightleftharpoons}} \text{Gas (soln)} \overset{k_{rxn}[\text{substrate(s)}]}{\rightleftharpoons} \text{Product} \qquad (8)$$

The rate of mass transfer is influenced by the surface area of the liquid exposed to the gas and the gas pressure (eq 9).

$$\frac{d[\text{gas}]}{dt} = k_L(\text{area}) \cdot p_{\text{gas}} \qquad (9)$$

Several factors influence the surface area of the liquid exposed

(10) For a discussion of mass-transfer-limitation effects in catalysis, see: Roberts, G. W. In *Catalysis in Organic Syntheses*; Rylander, P. N., Greenfield, H., Eds.; Academic Press: New York, 1976; pp 1−48.

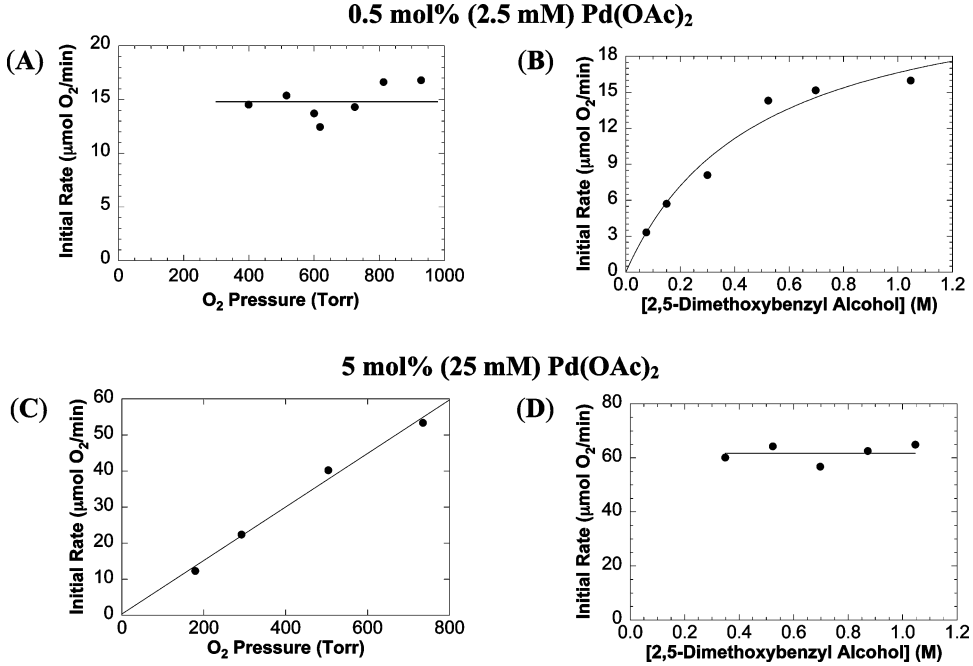

Figure 3. Dependence of the initial rate on oxygen pressure and alcohol concentration at both low and high catalyst loadings in the $Pd(OAc)_2$/DMSO-catalyzed aerobic oxidation of primary alcohol **1**. Conditions: (A) 2.5 mM $Pd(OAc)_2$, 399−913 Torr O_2, 0.52 M 2,5-dimethoxybenzyl alcohol, 2 mL of DMSO, 80 °C, in 25.4 mm OD tube; (B) 2.5 mM $Pd(OAc)_2$, 730 Torr O_2, 0.105−1.04 M 2,5-dimethoxybenzyl alcohol, 2 mL of DMSO, 80 °C, in 25.4 mm OD tube, data fit to a hyperbolic curve; (C) 25.2 mM $Pd(OAc)_2$, 179−735 Torr O_2, 520 mM 2,5-dimethoxybenzyl alcohol, 2 mL of DMSO, 80 °C, in 25.4 mm OD tube; (D) 24.9 mM $Pd(OAc)_2$, 725 Torr O_2, 0.349−1.05 M 2,5-dimethoxybenzyl alcohol, 2 mL of DMSO, 80 °C, in 25.4 mm OD tube, rates normalized to 1 atm.

Table 1. Measured Rates of O_2 Mass Transfer into DMSO at 80 °C Depending on Vessel Shape and Solution Volume[a]

reaction vessel	solution volume (mL)	maximum catalytic rate (μmol/min)
25 mL round-bottom flask	2.00	102.7 ± 9.1
25 mL round-bottom flask	5.00	98.5 ± 5.6
25.4 mm OD high-pressure tube	2.00	69.8 ± 7.4

[a] Reaction Conditions: 0.52 M **2**, 730 Torr O_2, 25 mM $Pd(OAc)_2$, DMSO, 80 °C.

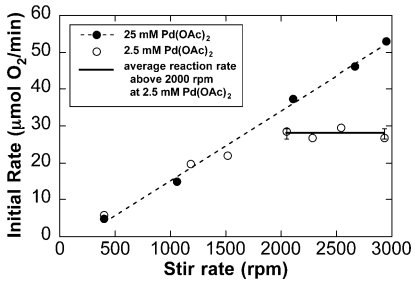

Figure 4. Dependence of the initial rate of $Pd(OAc)_2$/DMSO-catalyzed oxidation of **2** on the stirring speed. Conditions: (filled circles) 25.2 mM $Pd(OAc)_2$, 730 Torr O_2, 0.52 M 1-phenylethanol, 400−2950 rpm, 2 mL of DMSO, 80 °C, in 25.4 mm OD tube; (open circles) 2.5 mM $Pd(OAc)_2$, 730 Torr O_2, 0.52 M 1-phenylethanol, 400−2930 rpm, 2 mL of DMSO, 80 °C, in 25.4 mm OD tube.

to the gas-phase substrate, including the reactor design, solvent volume, and agitation rate. Use of the gas-uptake apparatus enabled us to obtain a direct measurement of the rate of oxygen gas dissolution into DMSO under catalytically relevant conditions. The data shown in Figure 5 reveal that 16 ± 1 μmol of dioxygen dissolves in 5.00 mL of DMSO in a 25 mL round-bottom flask. This solubility value of 3.2 ± 0.2 mM at 80 °C compares favorably to literature values ranging from 1.5 to 2.8

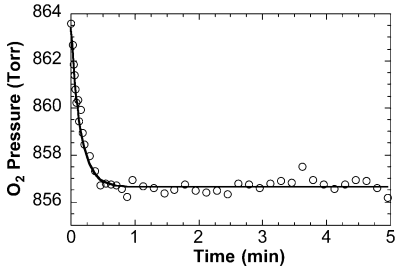

Figure 5. Measurement of the rate of oxygen gas dissolution into 5 mL of DMSO at 80 ° C. The curve-fit reflects a nonlinear least-squares fit to eq 10.

mM measured at lower temperature (25 °C).[11] The exponential fit of the data (eq 10, Figure 5)[12] provides a direct measurement of the rate of oxygen gas transfer into DMSO (85.4 ± 5.6 μmol/min).

$$P_t = P_{\text{final}} + (P_{\text{initial}} - P_{\text{final}}) \times \exp\left[\frac{-(P_{\text{initial}} - P_{\text{background}})\cdot k_L(\text{area})\cdot t}{P_{\text{final}} - P_{\text{background}}}\right] \quad (10)$$

To correlate these data with a mass-transfer-limited catalytic reaction, this oxygen dissolution rate was compared to the maximum rate measured for catalytic reactions carried out under the same conditions (5.00 mL DMSO, 80 °C, 25 mL round-bottom flask). The maximum catalytic rate (98.5 ± 5.6 μmol/min, Table 1) is within two standard deviations of the independently measured gas dissolution rate (Figure 6).

(11) (a) Gerrard, W. *Solubility of Gases and Liquids: A Graphic Approach. Data-Causes-Prediction*; Plenum Press: New York, 1976; p 24. (b) Achord, J. M.; Hussey, C. L. *Anal. Chem.* **1980**, *52*, 601−602. (c) Battino, R.; Rettich, T. R.; Tominaga, T. *J. Phys. Chem. Ref. Data* **1983**, *12*, 163−178.

(12) Deimling, A.; Karandikar, B. M.; Shah, Y. T.; Carr, N. L. *Chem. Eng. J.* **1984**, *29*, 127−140.

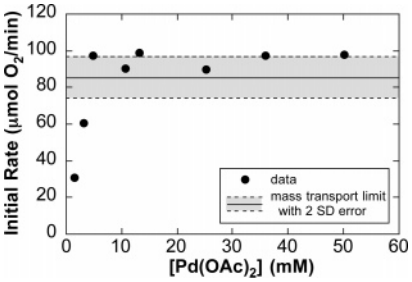

Figure 6. Dependence of the initial rate on [Pd(OAc)$_2$]. Conditions: 1.5−50.2 mM Pd(OAc)$_2$, 800 Torr O_2, 0.50 M 1-phenylethanol, 5 mL of DMSO, 80 °C, in round-bottom flask, rates normalized to 1 atm.

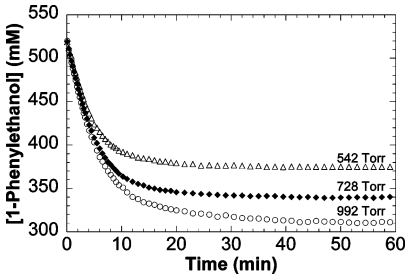

Figure 7. Reaction timecourses for the Pd(OAc)$_2$/DMSO-catalyzed oxidation of **2** at three different oxygen pressures. Conditions: 2.5 mM Pd(OAc)$_2$, 542−992 Torr O_2, 0.52 M 1-phenylethanol, 2 mL of DMSO, 80 °C, in 25.4 mm OD tube.

Oxygen Pressure Effects on Catalyst Decomposition. Mass-transfer effects are especially significant for palladium-catalyzed aerobic oxidation reactions because of the susceptibility of the reduced catalyst to decompose into inactive palladium metal. Thus, slow transfer of oxygen gas into solution not only affects the reaction rate but also contributes to catalyst decomposition. Catalyst decomposition also can be problematic under conditions that are not mass-transfer limited. At low [Pd(OAc)$_2$], the rate of alcohol oxidation exhibits virtually no dependence on the oxygen pressure (Figure 3A and Supporting Information Figure S1A). In Figure 7, the full-reaction timecourse is displayed for the Pd(OAc)$_2$/DMSO-catalyzed oxidation of the secondary alcohol **2** at three different oxygen gas pressures. Although the initial rates of the reactions are essentially identical (Figure 7 and Supporting Information Table S1), higher turnover numbers are evident at higher oxygen pressures (58, 72, and 84 turnovers are observed at initial oxygen pressures of 542, 728, and 992 Torr, respectively). This trend is readily rationalized by the mechanistic model in Scheme 1 whereby oxidation of the reduced catalyst competes directly with catalyst decomposition (step *ii* vs *iii*, Scheme 1). Although the present study has a mechanistic focus and, therefore, is not focused on optimization of the reaction, Sheldon et al. have reported high yields for palladium-catalyzed aerobic alcohol oxidation conducted in DMSO and H_2O/DMSO mixtures by employing 30 bar air pressure.[7f]

Catalyst Decomposition Pathways. Analysis of the [Pd(OAc)$_2$] Dependence Plots. The precise mechanism of catalyst decomposition is not known; however, the formation of catalytically inactive palladium black during the reactions suggests decomposition is associated with catalyst aggregation. Metal aggregation has been studied extensively in the context of colloid formation and nanoparticle synthesis, and both unimolecular and bimolecular pathways have been implicated in these processes.[13]

By analogy, catalyst decomposition in the present reactions could occur via both unimolecular and bimolecular pathways. Decomposition pathways that might exhibit a unimolecular dependence on [Pd(OAc)$_2$] include nucleation events associated with interactions between soluble Pd(0) and impurities in the solvent, the solvent itself, and/or the wall of the reaction vessel, for example. The most straightforward bimolecular decomposition mechanism is direct interaction of two Pd centers in a nucleation or particle-growth process. The kinetics of palladium decomposition (i.e., aggregation) have direct implications for catalyst performance.

Aerobic oxidation of the catalyst should exhibit a first-order dependence on [Pd] (e.g., rate = k_{ii}[Pd][O_2]).[14] If the catalyst decomposes via a unimolecular pathway, the first-order dependence of both catalytic turnover and catalyst decomposition (steps *ii* and *iii*, Scheme 1) will result in a *linear* dependence of the turnover rate on [Pd]. Such a trend is observed in the oxidation of the secondary alcohol **2** (inset, Figure 2). If decomposition proceeds via a bimolecular pathway, the decomposition rate will increase more rapidly than the catalytic rate at elevated [Pd] (i.e., $V_{cat} \propto [Pd]$; $V_{decomp} \propto [Pd]^2$). Therefore, the rate will exhibit a *nonlinear* dependence on the [Pd]. Such a trend is observed in the oxidation of the primary alcohol **1** (Figure 1A[15] and inset of Figure 1B).

The origin of the differences between the catalyst decomposition pathways in reactions involving primary and secondary alcohols cannot be discerned from the present study. Nevertheless, it is noteworthy that *the catalyst decomposition pathway is substrate dependent.* This observation may be related to the observation by Hiemstra and co-workers that colloidal palladium formed in Pd(OAc)$_2$/DMSO-catalyzed oxidative heterocyclization of alkenes (eq 11) retains catalytic activity.[3e] In contrast,

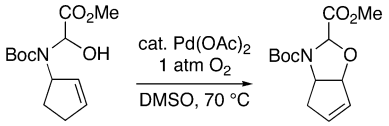

(11)

the aggregated palladium formed during alcohol oxidation is inactive. The enhanced catalyst stability in eq 11 appears to be a substrate- (or product-) induced phenomenon.

Catalyst Decomposition Pathways: Analysis of the Catalytic Reaction Timecourse Plots. Insights into the catalyst decomposition pathways were corroborated by evaluating the full timecourse of the reactions at different Pd(OAc)$_2$ concentrations. In the absence of mass-transfer effects, the rate of catalytic alcohol oxidation is approximately first order in [alcohol] at low to moderate concentrations (≤0.5 M) (cf. Figure 3B), and the rate law associated with this reaction (eqs 12 and 13) predicts that [alcohol] will exhibit an exponential decay with respect to time.[16] We recently observed such behavior, for example, in the Pd(OAc)$_2$/pyridine-catalyzed oxidation of 1-phenylethanol.[7c]

(13) For extensive references to this literature, see the following: (a) Watzky, M. A.; Finke, R. G. *J. Am. Chem. Soc.* **1997**, *119*, 10382−10400. (b) Besson, C.; Finney, E. E.; Finke, R. G. *J. Am. Chem. Soc.* **2005**, *127*, 8179−8184.

(14) Such a rate law has been observed for the aerobic oxidation of a well-defined Pd(0) complex, for example: Stahl, S. S.; Thorman, J. L.; Nelson, R. C.; Kozee, M. A. *J. Am. Chem. Soc.* **2001**, *123*, 7188−7189.

(15) In Figure 1A, only the highest [Pd] approaches the mass-transport-limit measure for a 25 mL round-bottom flask. The nonlinear [Pd(OAc)$_2$] dependence is therefore explained by invoking a higher-order (>1) dependence of the decomposition rate on [Pd].

$$\frac{d[R_2CHOH]}{dt} = k_i[R_2CHOH][Pd] \quad (12)$$

$$[R_2CHOH]_t = [R_2CHOH]_0 \exp(-k_i[Pd]_0 \cdot t) \quad (13)$$

If the catalyst decomposes during the course of the reaction, the concentration of active Pd catalyst will decrease and the rate will decrease proportionately. The effect of catalyst decomposition on the rate can be modeled by incorporating a time-dependent catalyst concentration term, $[Pd]_t$, into the original rate equation (eq 12). The identity of this term depends on whether decomposition proceeds via unimolecular or bimolecular process(es).[17] This treatment is elaborated in eqs 14−17 for the unimolecular decomposition pathway(s) and in eqs 18−21 for the bimolecular pathway(s). This analysis yields three separate integrated rate laws (eqs 13, 17, and 21) that can be used to evaluate the experimental timecourse data.

Rate law for unimolecular catalyst decomposition:

$$\frac{-d[Pd]}{dt} = k_{uni}[Pd] \quad (14)$$

Integrated rate law for unimolecular catalyst decomposition:

$$[Pd]_t = [Pd]_0 \exp(-k_{uni} \cdot t) \quad (15)$$

Incorporation of unimolecular catalyst decomposition term (eq 15) into catalytic rate law (eq 12):

$$\frac{d[R_2CHOH]}{dt} = k_i[R_2CHOH][Pd]_0 \exp(-k_{uni} \cdot t) \quad (16)$$

Integrated catalytic rate law incorporating unimolecular catalyst decomposition:

$$[R_2CHOH]_t = [R_2CHOH]_0 \exp\left[\frac{k_i[Pd]_0}{k_{uni}}(\exp[-k_{uni} \cdot t] - 1)\right] \quad (17)$$

Rate law for bimolecular catalyst decomposition:

$$\frac{-d[Pd]}{dt} = k_{bi}[Pd]^2 \quad (18)$$

Integrated rate law for bimolecular catalyst decomposition:

$$[Pd]_t = \frac{[Pd]_0}{1 + k_{bi}[Pd]_0 \cdot t} \quad (19)$$

Incorporation of bimolecular catalyst decomposition term (eq 19) into catalytic rate law (eq 12):

$$\frac{d[R_2CHOH]}{dt} = \frac{k_i[R_2CHOH][Pd]_0}{1 + k_{bi}[Pd]_0 \cdot t} \quad (20)$$

Integrated catalytic rate law incorporating bimolecular catalyst decomposition:

$$[R_2CHOH]_t = [R_2CHOH]_0(1 + k_{bi}[Pd]_0 \cdot t)^{-k_i/k_{bi}} \quad (21)$$

The full-reaction timecourses for the oxidation of **1** and **2** at different $[Pd(OAc)_2]$ highlight the detrimental influence of catalyst decomposition (Figures 8 and 9). None of the timecourse traces fit the exponential decay curve expected if no catalyst decomposition occurs, and in many cases, the reactions stop far short of full conversion.

Analysis of the timecourse traces for the oxidation of the primary alcohol **1** reveals that unimolecular Pd decomposition pathway(s) dominate at the lowest [Pd] tested (2.5 mM, Figure 8A); at higher [Pd], the unimolecular decomposition model is inadequate. At [Pd] = 5−12.5 mM, the timecourse traces fall between the simulated curves for unimolecular and bimolecular decomposition (Figure 8B and Supporting Information Figures S2−S4). It is reasonable to imagine that both unimolecular and bimolecular pathways are relevant in this [Pd] range. When [Pd] ≥ 15 mM, the timecourse fits are consistent with predominant bimolecular decomposition (Figure 8C,D). These timecourse-fitting results are consistent with the nonlinear dependence of the rate on $[Pd(OAc)_2]$ observed in the oxidation of **1** (Figure 1; see also the discussion in previous section).

The timecourse traces obtained for the oxidation of the secondary alcohol **2** differ from those obtained for the oxidation of **1**. Unimolecular catalyst decomposition pathway(s) appear to dominate until the $Pd(OAc)_2$ concentration is high enough to induce mass-transfer-limitation effects (Figure 9). At a $[Pd(OAc)_2]$ of 2.5, 5.0, and 10 mM, the rate equation associated with unimolecular decomposition (eq 17) fits the data well (Figure 9A−C). Only at $[Pd(OAc)_2]$ = 25 mM, a concentration at which mass-transfer-limitation effects are observed (Figure 2), does the bimolecular equation (eq 21) provide the appropriate fit (Figure 9D).[18] The unimolecular decomposition pathway that predominates in the oxidation of **2** is consistent with the linear dependence of the rate on $[Pd(OAc)_2]$ (inset, Figure 2).

Conclusions

Implications for the Palladium-Catalyzed Aerobic Oxidation Reactions. $Pd(OAc)_2$ in DMSO is among the most widely used catalyst systems for palladium-catalyzed aerobic oxidation of organic molecules. The present study provides a number of fundamental insights into this class of catalytic reactions, particularly associated with the influence of mass-transfer-limitation effects and catalyst decomposition pathways on the reactions. The insights gained from these studies and the methods described herein can also be applied to other palladium-catalyzed aerobic oxidation reactions.

The significant role of mass-transfer effects on $Pd(OAc)_2$/DMSO-catalyzed reactions undoubtedly reflects the low solubility of oxygen gas in DMSO. A number of common solvents are listed in Table 2, and among these examples, only water has lower oxygen solubility than DMSO. Although numerous

(16) Kinetic studies of the $Pd(OAc)_2$/pyridine-catalyzed reaction also reveal saturation dependence on [alcohol] (cf. Figure 3B); however, a first-order approximation for the [alcohol] dependence led to a very good exponential fit of the reaction timecourse.

(17) As we stated previously, the precise identity of these steps is not known, and it is reasonable to expect that multiple pathways might operate in parallel. Therefore, we treat all unimolecular (and bimolecular) processes collectively with a single phenomenological rate constant, k_{uni} (k_{bi}).

(18) It might be expected that a different set of rate equations would apply to reactions that exhibit mass-transfer-limitation effects because the rate is formally not dependent on the [alcohol] under these conditions. However, only the initial rate is limited by mass-transfer effects. Analysis of the timecourse data reveals that the reaction rate quickly falls below the mass-transfer limit (i.e., within the first few minutes), and >95% of the data is acquired under conditions that exhibit the typical [alcohol] dependence.

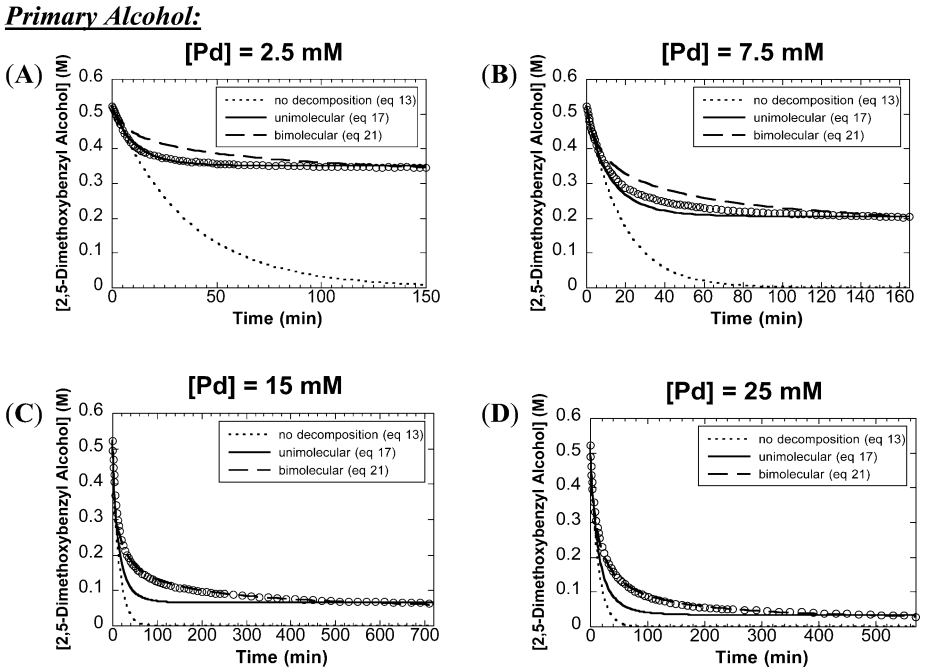

Figure 8. Representative timecourse of the oxidation of **1** with 2.5−25 mM $Pd(OAc)_2$. Initial and final time points were used to fit the timecourses to either a unimolecular decomposition equation (eq 17) or a bimolecular decomposition equation (eq 21). Only initial time points were used to fit the timecourse to an equation without a decomposition term (eq 13). Conditions: 2.5−25 mM $Pd(OAc)_2$, 730 Torr O_2, 0.52 M 2,5-dimethoxybenzyl alcohol, 2 mL of DMSO, 80 °C, in 25.4 mm OD tube.

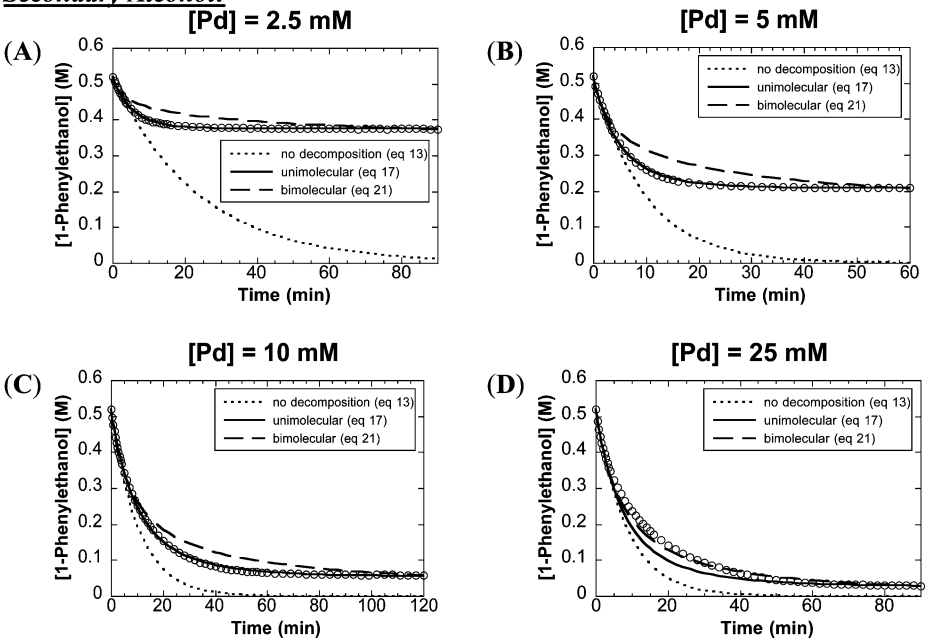

Figure 9. Representative timecourse of the oxidation of **2** with 2.5−25 mM $Pd(OAc)_2$. Initial and final time points were used to fit the timecourses to either a unimolecular decomposition equation (eq 17) or a bimolecular decomposition equation (eq 21). Only initial time points were used to fit the timecourse to an equation without a decomposition term (eq 13). Conditions: 2.5−25 mM $Pd(OAc)_2$, 730 Torr O_2, 0.52 M 1-phenylethanol, 2 mL of DMSO, 80 °C, in 25.4 mm OD tube.

factors are considered in the screening and development of new palladium catalyst systems for aerobic oxidation reactions, the role of oxygen solubility in the solvent is seldom explicitly discussed. Because of the intrinsic instability of palladium(0), it is necessary to ensure efficient reaction between dioxygen and the reduced palladium catalyst, even if this reaction is not the turnover-limiting step of the catalytic mechanism.[19] The presence of a high concentration of dissolved oxygen will play an important role in this process, and the use of a solvent with higher oxygen solubility may provide a convenient alternative to conducting the reaction at elevated gas pressures.[20]

Analysis of the catalytic timecourses implicates both unimolecular and bimolecular catalyst decomposition pathways. The bimolecular pathways can be minimized by reducing the catalyst

(19) This observation underlies our current interest in the effects of the catalyst coordination environment on the rates of palladium(0) oxygenation. See ref 14 and the following: Konnick, M. M.; Guzei, I. A.; Stahl, S. S. *J. Am. Chem. Soc.* **2004**, *126*, 10212−10213.

Table 2. Oxygen Gas Solubility in Common Solvents

solvent	O_2 solubility (mM)[a]	ref
perfluorobenzene	21.0	11c
n-hexane	15.7	11c
acetone	11.0	11b
chloroform	9.1[b]	11a
ethyl acetate	8.9[c]	11c
toluene	8.7	11c
acetonitrile	8.1	11b
N,*N*-dimethylformamide	4.5	11b
dimethyl sulfoxide	3.2[d]	this work
dimethyl sulfoxide	2.2	11c
H_2O	1.3	11c

[a] 25 °C unless otherwise indicated. [b] 16 °C. [c] 20 °C. [d] 80 °C.

concentration; however, the presence of unimolecular decomposition pathways places intrinsic limits on the catalyst lifetime. The analytical methods described above provide the foundation for future studies to investigate factors that contribute to improved catalyst stability.

Experimental Section

General Considerations. Palladium acetate (DuPont) was recrystallized prior to use from benzene/acetic acid.[21] Oxygen gas (BOC), 2,5-dimethoxybenzyl alcohol (Aldrich), 1-phenylethanol (Aldrich), benzene (Fisher), hexadecane (Aldrich), and anhydrous dimethyl sulfoxide (Aldrich) were used without purification. Gas chromatographic analysis of reactions was conducted with a Shimadzu GC-17A gas chromatograph with either a DB−Wax or a RTX-5 column.

Gas-Uptake Kinetics. A typical reaction was conducted as follows. $Pd(OAc)_2$ (11.2 mg, 50 μmol) was added to a 25 mL round-bottom flask with a stirbar. The flask was attached to an apparatus with a calibrated volume and a pressure transducer designed to measure the gas pressure within the sealed reaction vessel. The apparatus was evacuated to 200 Torr and filled with oxygen to 800 Torr, and this cycle was repeated 10 times. The pressure was established at 675 Torr. DMSO (1.85 mL) was added via syringe through a septum. The flask was heated to 80 °C. When the pressure stabilized in the apparatus, 2,5-dimethoxybenzyl alcohol (0.150 mL, 1.42 mmol) was added via syringe through a septum. Data were acquired using custom software written within LabVIEW (National Instruments). Correlations between oxygen uptake and conversion were made by analysis by gas chromatography with hexadecane as an internal standard.

Data-Fitting Procedure. Initial rates were determined from a linear fit to gas-uptake traces within the first 5% of substrate conversion. A typical data set and fit are shown in Supporting Information Figure S5, and analogous plots were used to obtain the data points shown in Figures 1−3 and 6. In some cases, pressure fluctuations arising from sample injections were evident in the first 10−20 s of the reactions; in such cases, these data points were not included in the fit.

Nonlinear least-squares fits of the timecourse data (Figures 8 and 9, Supporting Information Figures S2−S4) to various rate equations (eq 13, 17, or 21) were obtained by using the Solver function within Microsoft Excel. The exponential fits (perhaps better described as a simulation based on eq 13) correspond to an exponential extrapolation of the data acquired during the first 3 min of the reaction; the simulated data should fit the experimental data if no catalyst decomposition occurs. In the fits that account for catalyst decompostion (based on eq 17 or 21), the timecourse fit was initially optimized using the initial 3 min and the final 5 min of the reaction to ensure good starting and ending points. Subsequently, the entire timecourse was used to obtain a final fit. Rate constants obtained from the best fits to the data in Figures 8 and 9 and Supporting Information Figure S2 are provided in Table S2.

O_2 Dissolution in DMSO. For more precise measurements of the oxygen solubility, we increased the solution volume from 2 to 5 mL, which also dictated a change in vessel shape to allow better stirring. Oxygen dissolution measurements were made by heating DMSO to 80 °C under small amounts of nitrogen (around 30 Torr) in a vessel with known volume. A separate, but much smaller, vessel was pressurized to a high pressure of oxygen (around 8000 Torr). These vessels were connected through a solenoid valve, and when it was opened, the vessels quickly equilibrated to around 800 Torr. After equilibration, the solenoid valve was closed and stirring of the DMSO commenced.

Acknowledgment. We thank A. E. King for assistance in acquiring data for Figure 3A. This work was supported by the NIH (RO1 GM67173), the Dreyfus Foundation (Teacher-Scholar Award), and the Sloan Foundation (Research Fellowship).

Supporting Information Available: Additional kinetics plots and timecourse figures. This material is available free of charge via the Internet at http://pubs.acs.org.

JA057914B

(20) Safety is also a critical consideration in these reactions. In many cases, conditions that employ organic solvents with 1 atm of oxygen pressure fall within the explosive limits. Specific safety assessments generally must be conducted on a case-by-case basis.

(21) Stephenson, T. A.; Morehouse, S. M.; Powell, A. R.; Heffer, J. P.; Wilkinson, G. *J. Chem. Soc.* **1965**, 3632−3640.